ELSEVIER

19 February 1996

PHYSICS LETTERS A

Physics Letters A 211 (1996) 211–216

Global vector field reconstruction including a control parameter dependence

L. Le Sceller, C. Letellier, G. Gouesbet

Laboratoire d'Energétique des Systèmes et Procédés, URA CNRS 230, INSA de Rouen, BP 08, 76 131 Mont-Saint-Aignan, France

Received 19 July 1995; revised manuscript received 30 November 1995; accepted for publication 20 December 1995
Communicated by A.R. Bishop

Abstract

A global vector field reconstruction method including a control parameter dependence is derived and tested with the Rössler model. The reconstructed model is checked by comparing its bifurcation diagram with the one of the original system.

1. Introduction

Following pioneering papers by Packard et al. [1], Crutchfield and McNamara [2], and Farmer and Sidorowitch [3], global vector field reconstruction from numerical scalar time series has become a topic of growing interest in nonlinear dynamics (see Refs. [4–13]). In particular, the extraction of a set of equations which models experimental data is now a very important goal in the study of nonlinear systems (see Refs. [14–16]).

A global vector field reconstruction has already been applied to experimental systems by Brown et al. [16] with the times series provided by the Belousov–Zhabotinski reaction or by our group [14,15] with the experimental data coming from a copper electrodissolution (experimental setup by Hudson et al. [17]). A next step in data modelling is then to obtain a model which involves a control parameter dependence. Such a model has been obtained actually by using neural networks [18,19]. Nevertheless, a model involving a control parameter dependence was not yet given with a global vector field reconstruction method using a L_2-approximation. The aim of this paper is therefore to present a global vector field reconstruction technique allowing one to model the underlying physical system and its evolution under a control parameter modification from scalar time series recorded for different parameter values. The present work is a proof of principle. Extensions of the present work to experimental data and stability to noise are important issues that are postponed to future studies.

The paper is organized as follows. Section 2 describes the reconstruction method. Section 3 presents the reconstructed model with an explicit control parameter, starting from the variable y of the Rössler system. The model is checked by comparing the bifurcation diagram generated by the model with the one given by the Rössler system. Section 4 gives a conclusion.

2. Reconstruction method

Let us consider a nonlinear dynamical system defined by a set of autonomous ordinary differential

PII S0375-9601(96)00004-7

equations,

$$\dot{x} = f(x; \mu), \tag{1}$$

where $x(t) \in \mathbb{R}^n$ is a vector valued function depending on a parameter t called the time and f, the so-called vector field, is a n-component smooth function generating a flow ϕ_t. $\mu \in \mathbb{R}^p$ is the parameter vector with p components.

System (1) is called the original system and is unknown in the experimental cases. Without any loss of generality we present the method with $n = 3$. From an experimental point of view, only one variable is assumed to be known. Let this observable be called x. Let us also assume that we can record time series for different values of a recorded control parameter α. The original system may therefore be written as

$$\dot{x} = f_1(x, y, z, \alpha), \quad \dot{y} = f_2(x, y, z, \alpha),$$
$$\dot{z} = f_3(x, y, z, \alpha). \tag{2}$$

The aim now is to reconstruct a vector field equivalent to the original system in the form of a so-called standard system built on the observable and on its derivatives according to

$$\dot{X} = \dot{x} = Y, \quad \dot{Y} = Z, \quad \dot{Z} = F_s(X, Y, Z, \alpha), \tag{3}$$

where the reconstructed state space related to the standard system is spanned by derivative coordinates $(X, Y, Z) = (x, \dot{x}, \ddot{x})$

A global vector field reconstruction may then be achieved if a sufficiently good approximation $\tilde{F}_s$ of the so-called standard function F_s is designed. The approximation $\tilde{F}_s$ is obtained by using a Fourier expansion on a basis of orthonormal multivariate polynomials generated on the data set [7,13]. These polynomials depend on the derivative coordinates (X, Y, Z) and on the control parameter α, involving terms $(X^i Y^j Z^k \alpha^l)$, generalizing our previous studies without any control parameter in which monomials were more simply $(X^i Y^j Z^k)$. Therefore, we introduce monomials P^m,

$$P^m = X^i Y^j Z^k \alpha^l. \tag{4}$$

The one to one relationship used between quadruplets (i, j, k, l) and natural numbers m is an extension in four dimensions of the one defined in Ref. [13]. This relationship is clearly illustrated in Table 1.

Table 1
Relationship between quadruplets (i, j, k, l) and natural number m

m	(i, j, k, l)
1	(0, 0, 0, 0)
2	(1, 0, 0, 0)
3	(0, 1, 0, 0)
4	(0, 0, 1, 0)
5	(0, 0, 0, 1)
6	(2, 0, 0, 0)
7	(1, 1, 0, 0)
8	(1, 0, 1, 0)
9	(1, 0, 0, 1)
10	(0, 2, 0, 0)
11	(0, 1, 1, 0)
12	(0, 1, 0, 1)
13	(0, 0, 2, 0)
14	(0, 0, 1, 1)
15	(0, 0, 0, 2)
...	...

The approximation of the function may then be written as follows,

$$\tilde{F}_s = \sum_{m=1}^{N_m} K_m P^m, \tag{5}$$

where N_m is the dimension of the basis $\{P^m\}$. For a complete description of the approximation technique and for a better understanding of the present work, the reader may consult Ref. [13].

In this work, we arbitrarily choose to record the same number N_c of points x_i for each recorded value of the control parameter. It is then found that the reconstruction depends on (i) N_q, the number of vectors $(X_i, Y_i, Z_i, \dot{Z}_i, \alpha_i)$ $(i \in [1, N_q])$ on the net, (ii) h, the time step between each of them, (iii) N_s, the number of quadruplets $(X_i, Y_i, Z_i, \dot{Z}_i)$ sampled per pseudo-period for each recorded value of the control parameter, (iv) N_p, the number of retained multivariate polynomials and (v) p, the window size on which the derivatives are estimated. The vector $(N_c, N_q, h, N_s, N_p, p)$ is called the driving vector and defines all the reconstruction parameters. In practice, the choice of these parameters may have a significant effect on the quality of the results (see Refs. [13–15]).

A guideline for choosing a good driving vector is based on the use of an error function E_r which is defined as

$$E_r = \frac{\sum_{i=1}^{N_q} |\dot{Z}_i - \tilde{F}_s(X_i, Y_i, Z_i, \alpha_i)|}{\sum_{i=1}^{N_q} |\dot{Z}_i|}. \quad (6)$$

This error function is calculated by using absolute values for computational efficiency.

E_r may be understood as a relative error between the value of the standard function directly evaluated by calculating the fourth order derivative from the data series and the one obtained from its approximation. Let N_c and h be fixed from the available time series. For a given value of N_q, optimal values for N_s and the number of polynomials, N_p, are obtained by minimizing the error function. Therefore, the optimization problem reduces to finding a proper value of N_q. However, for a given N_q, the corresponding approximated system is not necessarily numerically integrable, even if the minimized error function passes through a minimum or a local minimum. Consequently, the search for a successful global vector field reconstruction needs systematical trials which can be automatically done with computational help.

For the global vector field reconstruction method developed here, the use of such an error function is very convenient. Nevertheless, finding an optimal modeling of nonlinear data series remains a tricky problem for which other research groups like Brown et al. [16] proposed more elaborate error functions. The use of such an error function is similar to the one of the least squares minimization term proposed by Brown et al. [16], and is very convenient for the global vector field reconstruction method developed here.

3. Application to the Rössler system

The Rössler system is a well known prototype of a continuous dynamical system defined by a nonlinear set of three ordinary derivative equations,

$$\dot{x} = -y - z, \quad \dot{y} = x + ay,$$
$$\dot{z} = b + z(x - c). \quad (7)$$

This system was extensively studied by our group along the following line in the control parameter space: $a \in [0.33, 0.557], b = 2., c = 4.$ [20,21]. Moreover, we have shown that there exists a diffeomorphism between the y-induced attractor and the original attractor [22]. Consequently, y provides a good checkpoint for our method. We choose y as the observable and a as the variable control parameter, (b, c) being fixed to $(2., 4.)$. For this observable, the exact standard function possesses a polynomial form and the standard system is

$$\dot{X} = \dot{y} = Y, \quad \dot{Y} = Z, \quad \dot{Z} = \sum_{m=1}^{51} K_m P^m, \quad (8)$$

where the K_m-coefficients are reported in Table 2.

This system is analytically derived since the original system is known. The model reconstructed by using the reconstruction method can be validated by comparison with this exact standard system. The learning set of data is composed of four time series $\{y_i, i \in [1, N_c = 1000]\}$, generated for four different values of the control parameter a taken to be equal to 0.2, 0.2625, 0.325 and 0.3875, respectively. One may remark that these a-values correspond to three different limit cycles of the period-doubling cascade and to a chaotic behaviour just beyond the accumulation point at $a_\infty = 0.386$. The sampling rate of the time series is taken according to the time step $h = 10^{-2}$. Successive derivatives up to the third order are estimated from the data. To this purpose, a sixth degree interpolating polynomial is built, centered at each point, by using the six nearest neighbours. Derivatives are then obtained by deriving these polynomials. The window size p is taken to be equal to 7 in terms of h.

A good approximation of the standard function is easily found with the driving vector $(1000, 100, 10^{-2}, 20, 51, 7)$ for which $E_r = 3.8 \times 10^{-7}$. With this driving vector, the estimated coefficients K_m^* of the standard function are reported in Table 2. The relative error ϵ between the exact coefficients K_m and the estimated coefficients K_m^* (for nonzero coefficients) is defined as

$$\epsilon = \frac{\sum_{i=1}^{N_m} |K_i - K_i^*|}{\sum_{i=1}^{N_m} |K_i|} \quad (9)$$

and is found to be less than 2.8%.

Integration of the reconstructed model gives attractors which may be shown to be topologically equivalent to the original Rössler attractors. For instance, the attractor obtained by integrating the reconstructed model for $a = 0.492$ is displayed in Fig 1. In order to

Table 2
Coefficients of the standard function: K_m are the values of the coefficients of the exact standard function F_s, K_m^* are the estimated values of K_m

m	K_m	K_m^*
1	−2.	−2.00097282
2	−4.	−3.99933339
3	−1.	−1.00003711
4	−4.	−3.999426
5	0.	0.00841346539
6	0.	-8.8697255×10^{-5}
7	1.	0.999894278
8	0.	−0.000214664992
9	0.	−0.00213157114
10	0.	7.51213253×10^{-5}
11	1.	0.999900554
12	4.	3.99972943
13	0.	-4.81485058×10^{-5}
14	1.	0.998381941
15	0.	−0.0221199429
16	0.	4.94222919×10^{-6}
17	0.	-7.78785747×10^{-6}
18	0.	1.19374657×10^{-5}
19	−1.	−0.999909364
20	0.	-7.04671011×10^{-6}
21	0.	-1.14912515×10^{-5}
22	0.	0.000396908727
23	0.	2.79227097×10^{-6}
24	−1.	−0.999482388
25	0.	0.00141280916
26	0.	3.00159042×10^{-6}
27	0.	-5.20397732×10^{-6}
28	−1.	−1.00019077
29	0.	8.66979364×10^{-8}
30	0.	0.000281140302
31	0.	0.000878615654
32	0.	-2.68477015×10^{-6}
33	0.	9.83049711×10^{-5}
34	0.	0.000670043193
35	0.	0.0180776258
36	0.	-1.30026484×10^{-6}
37	0.	-2.04684881×10^{-6}
38	0.	-2.72414197×10^{-6}
39	0.	3.08647232×10^{-7}
40	0.	2.01830313×10^{-6}
41	0.	-4.48262499×10^{-6}
42	0.	-1.62630908×10^{-5}
43	0.	-1.5198787×10^{-6}
44	0.	-3.12132332×10^{-6}
45	0.	0.000339325441
46	0.	-3.23923565×10^{-7}
47	0.	2.11870483×10^{-6}
48	0.	1.5706643×10^{-5}
49	0.	-2.45328909×10^{-6}
50	0.	-1.02050039×10^{-5}
51	1.	0.999712123

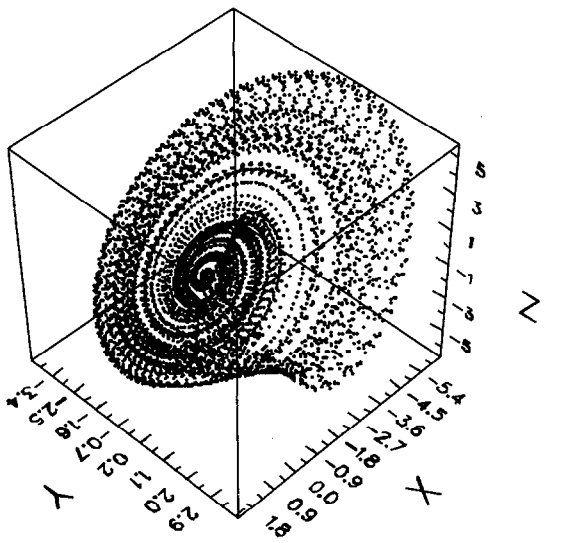

Fig. 1. Reconstructed attractor for $a = 0.492$.

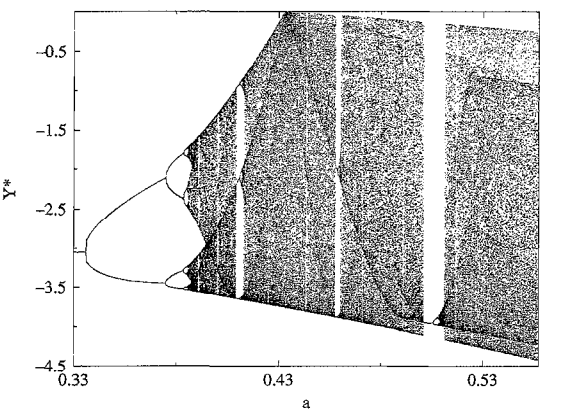

Fig. 2. Bifurcation diagram of the model reconstructed from the y-coordinate of the Rössler system.

check our model with respect to the control parameter dependence, let us now compare the bifurcation diagrams of the reconstructed system and of the standard exact system along the line $a \in [0.33, 0.557]$ (see Figs. 2 and 3). These diagrams are computed with the Y-coordinate of the trajectories crossing a Poincaré section P versus the values of the control parameter a, in which the Poincaré section P is defined as follows,

$$P = \{(Y, Z) \in \mathbb{R}^2 | X = X_-, \dot{X} > 0\}, \tag{10}$$

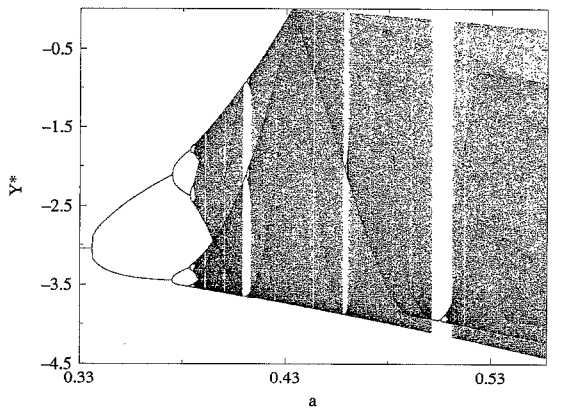

Fig. 3. Bifurcation diagram of the standard system derived from the Rössler system starting from the y-coordinate.

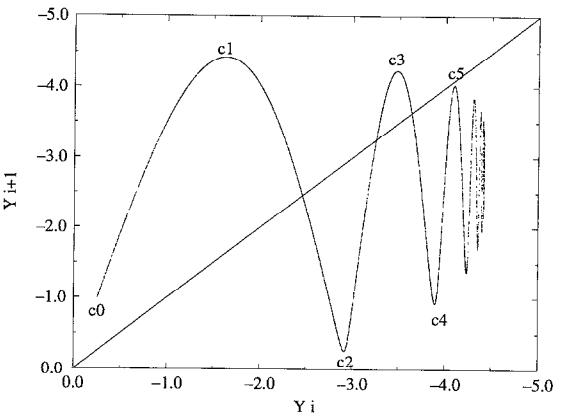

Fig. 4. First-return map in the Poincaré section P of the reconstructed model for $a = 0.5566334488$.

where $X_- = -[c - (c^2 - 4ab)^{1/2}]/2a$.

These two diagrams compare very favourably. The reconstructed model as well as the original system exhibit a period doubling scenario up to the accumulation point for $a_\infty = 0.386$. A chaotic behaviour is thereafter observed. The skeleton of periodic orbits which constitutes its spectrum evolves according to complex rules of growing and pruning providing a progressive enrichment of the phase portrait up to the death of the attractor for $a_D = 0.5566334488$.

The evolutions along the considered parameter space line $a \in [0.33, 0.557]$ of the two systems are now to be compared. This is achieved by computing first-return maps in the Poincaré section P giving a precise characterization of the dynamical behaviour of the Rössler system [21]. Between a_∞ and a_D, the first-return map of the standard system evolves from a two-branched map to a multi-branched map just before the boundary crisis that occurs at a_D [20]. For this a-value, the critical points are located according to a scaling law given by

$$\delta_c = \lim_{i\to\infty} \frac{Y_i - Y_{i-1}}{Y_{i+1} - Y_i} = 1.68 \pm 0.04, \qquad (11)$$

where the Y_i are the abscissae of the critical points c_i in the Poincaré section P of the exact standard system. This scaling property is identical to the one observed in the original system [20]. As shown in Ref. [20], a second scaling law is defined on the parameter values a_i for which new critical points c_i appear on the first-return map of the standard system. This scaling rule is [21]

$$\delta_a = \lim_{i\to\infty} \frac{a_i - a_{i-1}}{a_{i+1} - a_i} = 1.70 \pm 0.08. \qquad (12)$$

The parameter values a_i extracted from the standard system are reported in Table 3. Our reconstructed model is validated if it is found to be in agreement with these two scaling laws.

Indeed, the values of a_i^* found for the model are reported in Table 3 and are found to be very close to those observed on the standard system. As a result, the scaling factor δ_a^* is found to be

$$\delta_a^* = \lim_{i\to\infty} \frac{a_i^* - a_{i-1}^*}{a_{i+1}^* - a_i^*} = 1.70 \pm 0.08, \qquad (13)$$

in agreement with δ_a. Also, we find

$$\delta_c^* = \lim_{i\to\infty} \frac{Y_i^* - Y_{i-1}^*}{Y_{i+1}^* - Y_i^*} = 1.72 \pm 0.1, \qquad (14)$$

where the Y_i^* are the Y-coordinates of the critical points c_i^* on the first-return map in the Poincaré section P of the reconstructed system for $a = 0.5566334488$ (see Fig. 4), agreeing with δ_c. The reconstructed model is therefore checked.

4. Conclusion

We presented a global vector field reconstruction method allowing one to model the behaviour of physical systems under a control parameter evolution. This

Table 3
Successive a-values for which a new critical point c_i appears on the first-return map of the Poincaré section of the standard system. The values a_i^* observed for the reconstructed model, also reported, are found to be in very good agreement with the exact values

c_i	a_i	a_i^*
c_0	0.432909 1	0.432909
c_3	0.491 22	0.491 3
c_4	0.523 85	0.523 85
c_5	0.537 525	0.537 525
c_6	0.546 220 77	0.546 220 77
c_7	0.550 384 86	0.550 384 86
c_8	0.553 089 50	0.553 089 50
c_9	0.554 486 01	0.554 486 01
c_a	0.555 390 91	0.555 390 91
c_b	0.555 878 95	0.555 878 90
c_c	0.556 192 09	0.556 192 09
c_d	0.556 365 68	0.556 365 68
c_e	0.556 475 85	0.556 475 85
c_f	0.556 537 984	0.556 537 9
c_g	0.556 577 029	0.556 577 029
c_h	0.556 599 350	0.556 599 320
c_i	0.556 613 243	0.556 613
c_j	0.556 621 282	0.556 621 2
c_∞	0.556 633 448 8	0.556 633 448 8

method has been successfully applied for the Rössler system starting from y-time series. This technique permits one to predict behaviour and bifurcations of the original system for control parameter values for which the system has not been observed. We now have to test this method on experimental data series and, particularly, to check if its prediction capacities are robust against noise perturbations.

References

[1] N.H. Packard, J.P. Crutchfield, J.D. Farmer and R.S. Shaw, Phys. Rev. Lett. 45 (1980) 712.
[2] J.P. Crutchfield and B.S. McNamara, Complex Systems 1 (1987) 417.
[3] J.D. Farmer and J.J. Sidorowich, Phys. Rev. Lett. 59 (1987) 845.
[4] A.K. Agarwal, D.P. Ahalpara, P.K. Kaw, H.R. Prablakera and A. Sen, J. Phys., 35 (1990) 287.
[5] J.L. Breeden and A. Hübler, Phys. Rev. A 42 (1990) 5817.
[6] M. Casdagli, S. Eubank, J.D. Farmer and J. Gibson, Physica D 51 (1991) 52.
[7] M. Giona, F. Lendini and V. Cimagalli, Phys. Rev. A 44 (1991) 3496.
[8] G. Gouesbet, Phys. Rev. A 43 (1991) 5321.
[9] G. Gouesbet, Phys. Rev. A 44 (1991) 6264.
[10] M. Palus and I. Dvoràck, Physica D 55 (1992) 221.
[11] G. Gouesbet, Phys. Rev. A 46 (1992) 1784.
[12] G. Gouesbet and J. Maquet, Physica D 58 (1992) 202.
[13] G. Gouesbet and C. Letellier, Phys. Rev. E 49 (1994) 4955.
[14] C. Letellier, L. Le Sceller, E. Maréchal, P. Dutertre, B. Maheu, G. Gouesbet, Z. Fei and J.L. Hudson, Phys. Rev. E 51 (1995) 4262.
[15] C. Letellier, L. Le Sceller, P. Dutertre, G. Gouesbet, Z. Fei and J.L. Hudson, J. Phys. Chem., to be published.
[16] R. Brown, N.F. Rulkov and E.R. Tracy, Phys. Rev. E 49 (1995) 3784.
[17] Z. Fei, J.L. Hudson and R.G. Kelly, J. Electrochem. Soc. 141 (1994) L123.
[18] R. Rico-Martínez, K Krischer, I.G. Kevrekidis, M.C. Kube and J.L. Hudson, Chem. Eng. Commun. 118 (1992) 25.
[19] A.S. Lapedes and R.B. Farber, Los Alamos Report LA-UR, 87-2662 (1987).
[20] C. Letellier, P. Dutertre and B. Maheu, Chaos 5 (1995) 271.
[21] P. Dutertre, Caractérisation des attracteurs à l'aide d'orbites périodiques, Ph.D. thesis, LESP, URA CNRS 230, Rouen (1995).
[22] C. Letellier and G. Gouesbet, Equivalences between original and reconstructed strange attractors in the case of 3D differential embeddings, submitted to Chaos.